Front. Optoelectron. China 2009, 2(1): 40–49
DOI 10.1007/s12200-009-0007-y

RESEARCH ARTICLE

All-optical ultra-wideband pulse generation based on semiconductor optical amplifiers

Jianji DONG, Xinliang ZHANG (✉), Dexiu HUANG

Wuhan National Laboratory for Optoelectronics, School of Optoelectronic Science and Engineering, Huazhong University of Science and Technology, Wuhan 430074, China

Abstract Several all-optical methods for ultra-wideband (UWB) pulse generation based on various nonlinearities of single semiconductor optical amplifiers (SOAs), namely cross phase modulation (XPM), cross gain modulation (XGM), and a hybrid of self phase modulation (SPM) and XGM, have been demonstrated. In the first method, UWB doublet pulses are realized with XPM. The input optical Gaussian pulse will be converted to two polarity-reversed monocycle pulses by a blue shifted and a red shifted optical bandpass filters respectively. These two monocycle pulses are then combined with proper time delay to generate two polarity-reversed doublet pulses. Second, two polarity-reversed monocycle pulses are obtained based on XGM of the SOA and group delay of the single mode fiber (SMF). In the scheme, two polarity-reversed Gaussian pulses are generated due to XGM, and then the mixed signal is converted to a monocycle shape due to the group delay of the SMF. Finally, we present UWB doublet generation based on SPM. The monocycle pulse is generated from a dark return-to-zero (RZ) signal and converted to a doublet pulse by injecting an additional probe signal with the SMF transmission. For the first time and to the best of our knowledge, we report that the generated doublet pulses are transmitted over 5 km SMF by proper dispersion compensation without distortion. The configuration of our all-optical methods is compact and simple. The feasibility to implement the pulse shape modulation and pulse polarity modulation is discussed.

Keywords microwave photonics, ultra-wideband (UWB), semiconductor optical amplifier (SOA), all-optical microwave signal processing

Received April 10, 2008; accepted May 30, 2008

E-mail: xlzhang@mail.hust.edu.cn

1 Introduction

Ultra-widebands (UWBs) are regulated by the Federal Communications Commission (FCC) and draw considerable attention for a variety of applications, including communication, imaging, surveillance, and locating. One of the most attractive applications is for the indoor communication system [1]. UWB technology has many advantages over traditional wireless communication, including lower power consumption, higher bit rate, immunity to multipath fading, shorter time duration, and lower duty cycle [2,3]. The FCC also defines UWB as any signal that occupies more than 500 MHz of bandwidth in the 3.1 to 10.6 GHz band or has a fractional bandwidth greater than 20%.

The choice of UWB pulse types is critical to the performance of UWB systems. The Gaussian monocycle and doublet pulses are the first-order and second-order derivative of a Gaussian pulse, which have been considered promising candidates for UWB communications [4]. Many approaches to generating UWB signals are implemented using electronic circuits in the electrical domain [5–7]. However, with the current stage of technology, it is difficult and expensive to generate UWB pulses with a large fractional bandwidth. In addition, current UWB signals are limited to short distances due to low power density, whereas UWB-over-fiber technology can provide a promising solution to integrate the local UWB environment into the fixed wired optical network or wireless wide-area infrastructures [8]. Therefore, it is highly desirable that UWB signals be generated directly in an optical domain without electrical-optical conversion so that optical advantages such as huge bandwidth capacity and immunity to electromagnetic interference can be utilized.

Generally, UWB generation in an optical domain can be grouped into two categories: hybrid method and all-optical method. Figure 1 shows a conceptual illustration of a typical UWB-over-fiber system, where the UWB signal is generated by both methods. In the system, optical UWB pulses are generated and encoded in the central office, transmitted by the fiber link, and distributed to the access point. Use of the hybrid method means that the input pulse is generated electrically and the UWB pulse is generated by optical devices, while use of the all-optical method means that both the input pulse and output UWB pulse are generated in the optical domain. The all-optical schemes can be easily incorporated into UWB-over-fiber networks and eventually simplify the entire network. The hybrid methods to generate UWB signals are reported with microwave differentiators [9], optical phase modulators [10–13], chirp-to-intensity converters [10,14], intensity modulators [15–17], and photonic microwave delay-line filters [18]. The all-optical methods are reported with semiconductor optical amplifiers (SOAs) [19–22], dispersion shifted fibers [23], and frequency to time mapping technology [24]. Among these techniques, the SOA is one of the most promising candidates for all-optical UWB generation due to high nonlinearities, optically-controlled manipulation, small footprint, and low power consumption. In a practical UWB-over-fiber network, UWB pulse encoding techniques such as pulse polarity modulation (PPM) and pulse shape modulation (PSM) are also very important. The PPM means modulating the UWB pulse with different polarities, and the PSM means modulating the UWB pulse with different shapes, such as monocycle-doublet conversion. Wang et al. demonstrated the PPM of UWB monocycle and doublet pulses by rotating the polarization state of incident light to the polarization modulator [25].

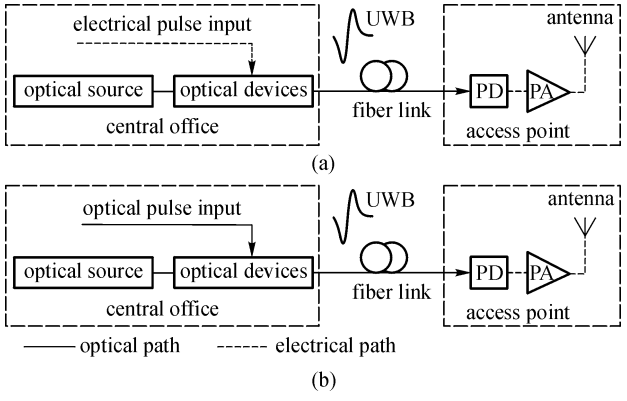

Fig. 1 Comparison of different methods to generate optical UWB signals. (a) Hybrid method for UWB generation; (b) all-optical UWB generation (LD: laser diode; PD: photodetector; PA: power amplifier)

In this paper, we present several all-optical methods for UWB generation based on various nonlinear effects of a single SOA. First, UWB doublet pulses are realized with cross phase modulation (XPM) of the SOA, which serves as an all-optical phase modulator. The input optical Gaussian pulse will be converted to two polarity-reversed monocycle pulses by a blue shifted optical bandpass filter (OBF) and a red shifted OBF respectively. These two monocycle pulses are then combined with proper time delay to generate two polarity-reversed doublet pulses. Second, a pair of polarity-reversed monocycle pulses is obtained based on cross gain modulation (XGM) of the SOA and group delay of a section of single mode fiber (SMF). A pair of inverted and positive Gaussian pulses is generated due to XGM in the pump-probe scheme, and then the mixed signal is converted to monocycle shape due to the group delay of the SMF. The polarity and pulse width of monocycle pulses are dependent on the group delay. Third, we present UWB doublet generation based on self phase modulation (SPM) of the SOA. When an optical signal with dark return-to-zero (RZ) format propagates through the SOA, the output pulses will become monocycle-like due to the overshoot at the rising edges. The monocycle pulse can be converted to a doublet pulse by injecting an additional probe signal with the SMF transmission. For the first time and to best of our knowledge, we report that the generated doublet pulses are transmitted over 5 km SMF by proper dispersion compensation without distortion. The radio frequency (RF) spectra of all generated UWB pulses conform to the FCC's UWB definition. The configuration of our all-optical methods is compact and simple. The feasibility to implement the PSM and PPM is also discussed.

2 All-optical UWB doublet generation based on XPM

In Ref. [20], we presented UWB monocycle generation by XPM of SOA. Here we extend the previous work and demonstrate a UWB doublet generation method. The operation principle of all-optical UWB doublet generation is shown in Fig. 2. A probe light with continuous wave (CW) is generated by the first laser diode (LD 1), and an optical Gaussian pulse is generated by LD 2. The normalized Gaussian pulse train can be expressed in the form

$$P_s(t) = \sum_{n=-\infty}^{+\infty} \Omega(t - nT_r), \tag{1}$$

where $\Omega(t)$ represents an ideal Gaussian pulse waveform and T_r is the pulse repetition interval. When the Gaussian pulses and the probe signal are simultaneously injected into the SOA, the probe signal will experience both XGM and XPM, and the temporal phase Φ_c will keep changing approximately in proportion to $P_s(t)$. The phase of the probe signal can then be written as

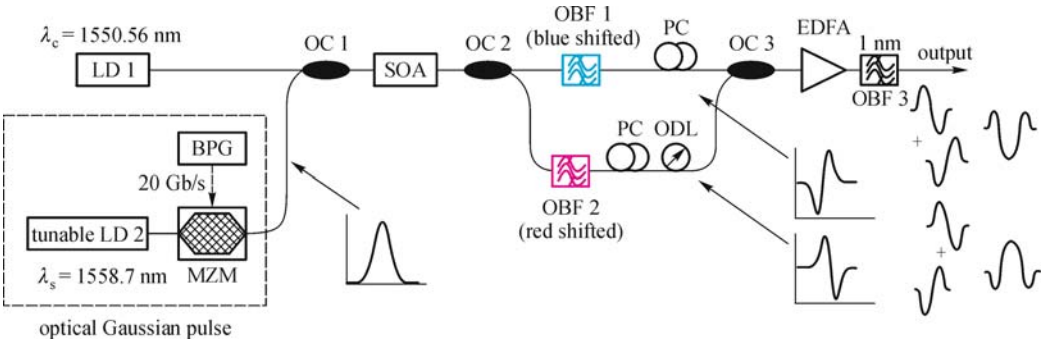

Fig. 2 Experimental setup for all-optical UWB generation based on XPM scheme (BPG: bit pattern generator; OC: optical coupler; MZM: Mach-Zehnder modulator; EDFA: erbium-doped fiber amplifier; OBF: optical bandpass filter; ODL: optical delay line; PC: polarization controller)

$$\Phi_c(t) = KP_s(t) + \Phi_0, \tag{2}$$

where K is the proportional constant and Φ_0 is the initial phase.

The chirp of the probe signal is the first order derivative of the phase, which is expressed as

$$\Delta\nu_c(t) = -\frac{1}{2\pi}\frac{d\Phi_c(t)}{dt} = -\frac{K}{2\pi}\frac{dP_s(t)}{dt}. \tag{3}$$

From Eq. (3), we know that the chirp has a monocycle shape, which is the first order derivative of the Gaussian pulse. The temporal chirp is the frequency shift of the probe signal, and its positive/negative value represents blue/red shift of the probe wavelength.

The SOA is followed by a Gaussian OBF. Figure 3 shows the transfer function of the Gaussian OBF, where point B presents the filter's central wavelength, marked as λ_f. If the probe wavelength λ_c is within the filter's linear region (point A in Fig. 3), namely $\lambda_f = \lambda_c + \Delta\lambda_{det}$, the output pulse will assume a monocycle shape. Due to the symmetry of the transfer function, the output pulse will be a polarity-reversed monocycle if the probe carrier is located on the negative slope of the filter's transmission spectrum (point C in Fig. 3). To be more explicit, the monocycle at point C is considered a negative one, while at point A is considered positive. Since two polarity-reversed UWB monocycle pulses can be generated by two OBFs with opposite detuning to the probe carrier, one can combine this pair of monocycle pulses with proper time delay to obtain two polarity-reserved UWB doublet pulses, as shown in Fig. 2.

The experimental setup is also described in Fig. 2. The probe signal is generated by LD 1 at 1550.56 nm with 1 mW output power. Another tunable laser diode (LD 2) emits CW light at 1558.7 nm, which is modulated by the Mach-Zehnder modulator (MZM) to form optical Gaussian pulses. The bit pattern generator (BPG) drives the MZM at a repetition rate of 20 Gb/s with a fixed pattern "1000 0000 0000 0000" (one "1" per 16 bits), which is equivalent to a

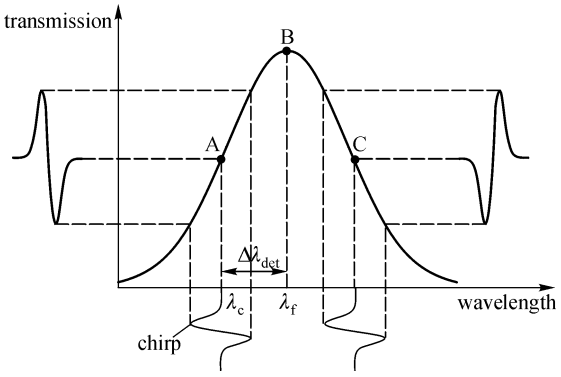

Fig. 3 Chirp-amplitude conversion with Gaussian OBF

Gaussian pulse train with a repetition rate of 1.25 GHz. The Gaussian pulse has a duty cycle of about 1/16 and full width at half maximum (FWHM) of about 50 ps. The optical Gaussian pulses have a peak power of 2.5 mW. The SOA (Kamelian NL-SOA) is biased at 200 mA, and the polarization dependence gain is less than 1 dB. The SOA output signal is split into two beams by the optical coupler (OC 2). The two beams are followed by two tunable OBFs with the same series (Santec-OTF-0 M) respectively. The OBFs have a 3-dB bandwidth of 0.32 nm and an insertion loss of 5 dB. The OBF 1 is blue shifted with respect to the probe wavelength to get the negative monocycle, and the OBF 2 is red shifted to get the positive one. The optical delay line (ODL) ensures the combination of two polarity-reserved monocycle pulses with proper time delay. The polarization controller (PC) is used to eliminate the interference. Due to the large loss of OBFs, an erbium-doped fiber amplifier (EDFA) is used to amplify the output power. Another OBF 3 with 1 nm bandwidth is used to suppress the amplified spontaneous emission (ASE) noise. The output optical signal is measured by a high speed sampling oscilloscope (Tektronix CSA8000B). The radio frequency (RF) spectrum is calculated via fast Fourier transform method [26], which is equivalent to the measurement data of the RF analyzer. UWB doublet

pulses will be obtained by combining the positive and negative monocycle pulses with proper delay.

To investigate the relative wavelength shifts of the probe signal, we fix the probe wavelength at 1550.56 nm and adjust the central wavelength of OBF 1. The OBF 2 is switched off. First, the OBF 1 is blue shifted by 0.4 nm to locate the probe wavelength on the negative slope of OBF 1, as shown in Fig. 4. We obtain the waveform of negative monocycle pulses, as shown in Fig. 5(a). The upper FWHM is about 50 ps, while the lower FWHM is about 74 ps. Figure 5(b) shows the RF spectrum of the monocycle pulse signal. The central frequency is defined as the peak frequency, while the 10 dB bandwidth is defined as the frequency range of 10 dB reduction from the

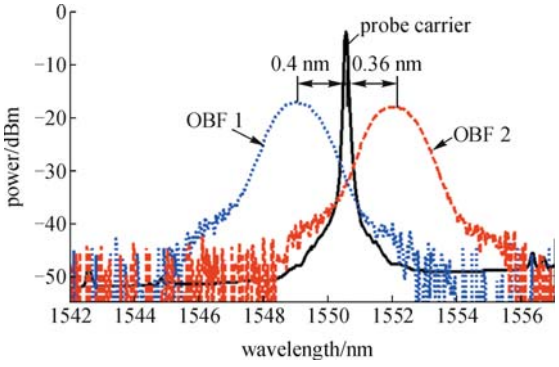

Fig. 4 Transmission spectrum of OBF 1 and OBF 2. Probe carrier is located on the slope of OBF spectrum

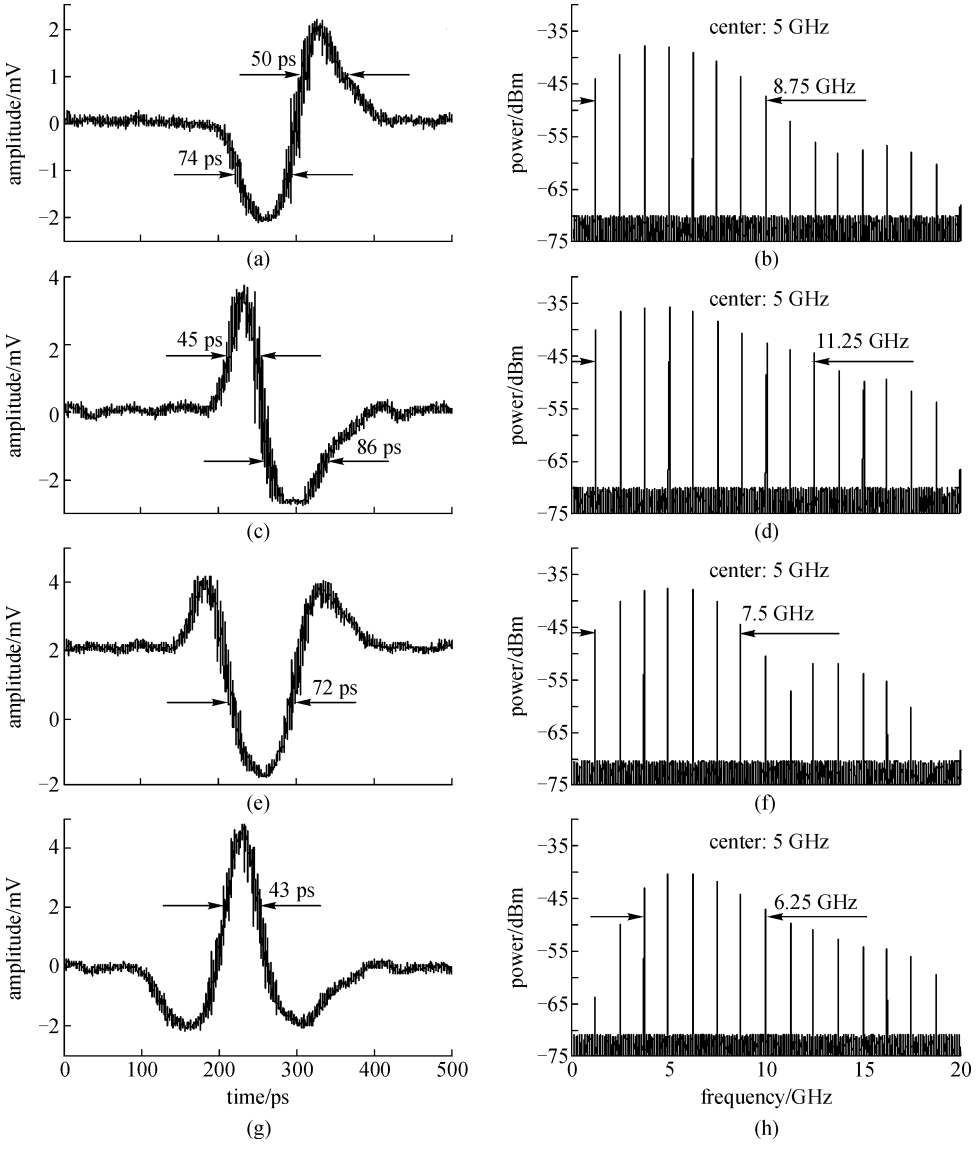

Fig. 5 Measured UWB pulses and their RF spectra. (a) Negative monocycle pulse with blue shifted OBF 1; (b) RF spectrum with blue shifted OBF 1; (c) positive monocycle pulse with red shifted OBF 2; (d) RF spectrum with red shifted OBF 2; (e) doublet pulse (positive monocycle pulse is 50 ps earlier than the negative one); (f) RF spectrum (positive monocycle pulse is 50 ps earlier than the negative one); (g) doublet pulse (positive monocycle pulse is 100 ps later than the negative one); (h) RF spectrum (positive monocycle pulse is 100 ps later than the negative one)

peak frequency. After the reduction, the central frequency is 5 GHz, and the 10 dB bandwidth is about 8.75 GHz (from 1.25 to 10 GHz). This means that the generated monocycle pulse has a fractional bandwidth of 175%. In addition, the frequency spacing between two neighboring lines is 1.25 GHz, which equals the repetition rate of the monocycle pulse train.

The central wavelength of the OBF 2 is now tuned at 1550.92 nm and the OBF 1 is switched off. In such a case, the probe wavelength is located on the positive slope of OBF 2, as shown in Fig. 4, and the output pulse assumes a positive monocycle shape which is inverted from the previous one. The waveform of the monocycle pulses is shown in Fig. 5(c). We measured the upper FWHM and lower FWHM, which are 45 and 86 ps, respectively. Figure 5(d) shows the RF spectrum of the positive monocycle. After the measurement, the central frequency is 5 GHz, and the 10 dB bandwidth is 11.25 GHz.

Therefore, we have demonstrated two polarity-reversed monocycle pulse generations with blue shifted OBF 1 and red shifted OBF 2. Both OBF 1 and OBF 2 are switched on to obtain a pair of UWB doublet pulses with reversed polarities. When the ODL is properly adjusted so that the positive monocycle pulse is 50 ps earlier than the negative one, we obtained the doublet pulse, as shown in Fig. 5(e). The FWHM is 72 ps. Figure 5(f) shows the RF spectrum of generated doublet pulses. After the measurement, the central frequency is 5 GHz, and the 10 dB bandwidth is 7.5 GHz. Conversely, when the positive monocycle pulse is 100 ps later than the negative one, we obtain another doublet pulse with reversed polarity, as shown in Fig. 5(g). Figure 5(h) shows the RF spectrum of generated doublet pulses. After the measurement, the central frequency is 5 GHz, and the 10 dB bandwidth is 6.25 GHz. The RF spectra in Fig. 5 matches the UWB definition of the FCC.

In conclusion, a pair of monocycle pulses and a pair of doublet pulses with opposite polarity are obtained. This feature provides the potential function of PPM and PSM. For PPM of monocycle pulses, one can switch either the probe wavelength or the OBF central wavelength so that the probe carrier is switched between the positive and negative OBF slope. For PPM of doublet pulses, one can use an electrically controlled ODL to switch the polarity of doublet pulses, and both the probe wavelength and OBF central wavelength are fixed. The PSM is also possible. For example, the monocycle-doublet conversion can be implemented when the red shifted OBF 2 is switched from off to on, and vice versa.

3 All-optical UWB pulse generation based on XGM

The technique to generate UWB pulses discussed in Sect. 2 requires at least two OBFs and an additional EDFA. These additional optical devices make the system rather costly. Since two polarity-reversed pulses can be obtained with a pump-probe scheme due to XGM in the SOA, one can combine the pump and probe wavelengths with proper time delay to generate a UWB monocycle pulse. Unlike the method of Ref. [19], which is based on cascaded fiber Bragg gratings (FBGs), our aim is to make the system filter-free and compact. Our previous work demonstrated a filter-free approach to generating UWB monocycle pulses [22]. The monocycle is automatically generated without optical filters and ODL. However, only a positive monocycle can be generated and the FWHM of monocycle pulses is difficult to change. In this section, we propose a filter-free, pump-probe scheme to generate a pair of polarity-reversed monocycle pulses based on XGM in the SOA and the SMF dispersion. Moreover, the FWHM of monocycle pulses can be easily changed by the wavelength span of pump and probe signals or the length of SMF.

Figure 6 shows the operational principle of a filter-free UWB generation scheme. Configured as a traditional pump-probe scheme, a CW probe light at λ_c and optical Gaussian pulse train at wavelength λ_s are launched into the SOA simultaneously [see Figs. 6(a) and 6(b)]. Due to XGM in the SOA, the CW probe signal obtains an inverted Gaussian shape [see Fig. 6(c)]. Because of non-uniform amplification, the Gaussian pulse after the SOA becomes sharp at its leading edge so that the power peak is shifted forward [see Fig. 6(d)]. The pulse distortion is beneficial to our scheme since it effectively avoids power cancellation of the amplified Gaussian pulse and polarity-reversed probe light. Hence, the peak of the Gaussian pulse and the pit of probe light at the SOA output are misaligned temporarily. As a result, the mixed signal assumes a monocycle shape without optical filter and time delay. Since the monocycle pulse is the first-order derivative of a Gaussian pulse, our scheme has been successfully applied to an all-optical intensity differentiator [27]. A section of SMF following the SOA serves as the dispersion medium to effect a proper group delay between the Gaussian pulse and the inverted probe light. The group delay is expressed as

$$\Delta t = D(\lambda_c - \lambda_s)L, \tag{4}$$

where D is the dispersion parameter and L is the SMF length. Both positive and negative monocycle pulses can be generated if Δt is positive and negative respectively, as shown in Fig. 6(e).

The experimental setup is described in Fig. 6. LD 1 emits an optical signal at 1558.72 nm, which is modulated by MZM to generate an optical Gaussian pulse. The optical Gaussian pulse has a repetition rate of 1.25 GHz and a FWHM of 70 ps. Tunable LD 2 emits a probe signal at 1556.64 nm. Two attenuators (ATTs) are used to adjust the input power of the SOA. The employed SOA is the same as that in Sect. 2. The gain recovery time is 60 ps. The SOA is biased at 200 mA. The consequent SMF has a

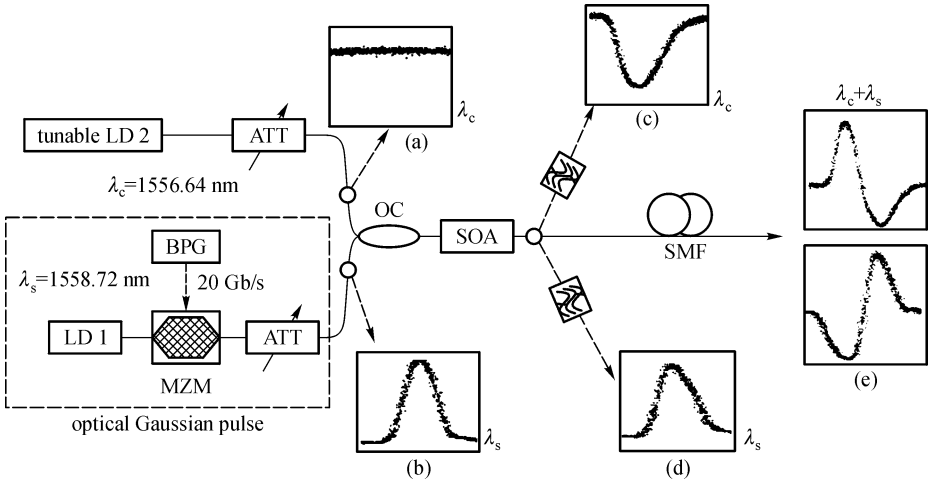

Fig. 6 Experimental setup for filter-free UWB generation based on XGM scheme. (a) Input probe; (b) input Gaussian pulse; (c) output probe after SOA; (d) output Gaussian pulse after SOA; (e) mixed signal after SMF

length of 2.5 km with $D = 17$ ps/(nm·km) and the group delay $\Delta t = -88.4$ ps.

When peak power of the Gaussian pulse and the probe power are 3 and 0.5 mW respectively, we observe a positive monocycle pulse at the SOA output, as shown in Fig. 7(a). The upper FWHM and lower FWHM are 50 and 65 ps, respectively. Figure 7(b) shows the corresponding RF spectrum, which reveals that the central frequency is 5 GHz, and the 10 dB bandwidth is 8.75 GHz. The mixed signal is then transmitted in the SMF, and the group

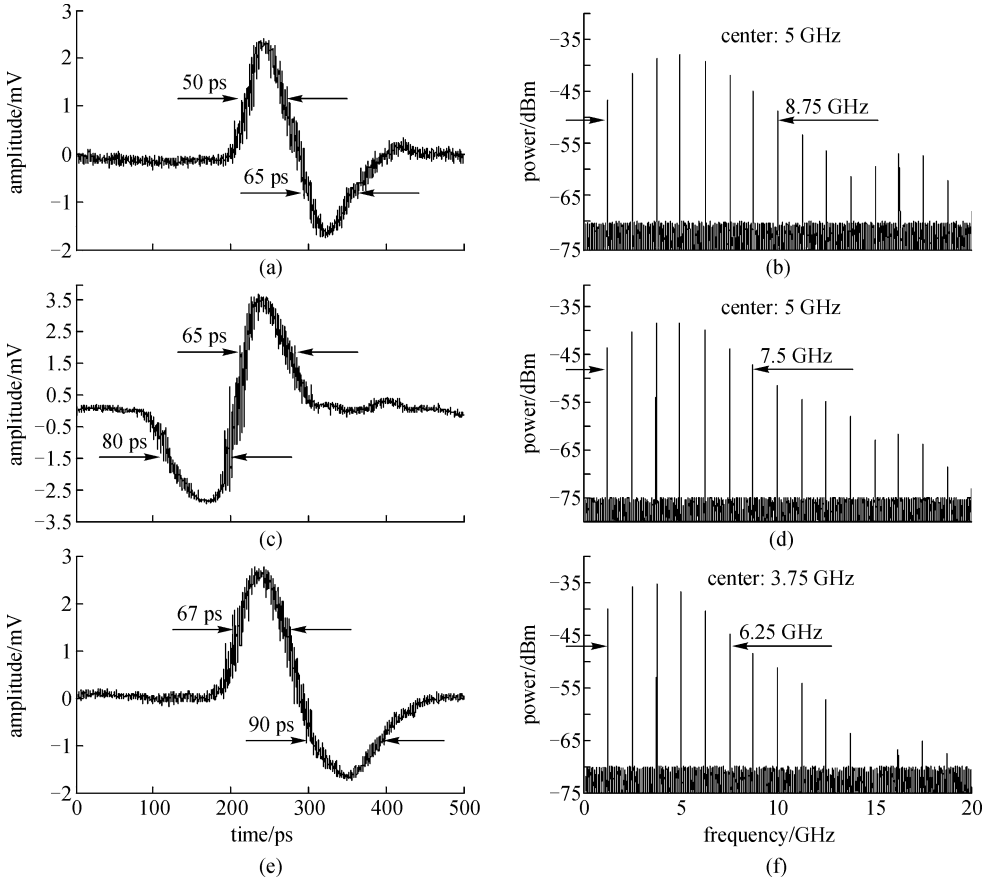

Fig. 7 Measured UWB waveforms and RF spectra. (a) Positive monocycle pulse without SMF transmission; (b) RF spectrum without SMF transmission; (c) negative monocycle pulse ($\Delta t = -88.4$ ps); (d) RF spectrum ($\Delta t = -88.4$ ps); (e) positive monocycle pulse ($\Delta t = 85$ ps); (f) RF spectrum ($\Delta t = 85$ ps)

delay is −88.4 ps. This means that the inverted probe light is 88.4 ps earlier than the Gaussian pulse. The mixed signal turns into a negative monocycle pulse, as shown in Fig. 7(c). The upper/lower FWHM is 65 ps/80 ps. Figure 7(d) shows the RF spectrum. After the measurement, the central frequency and the 10 dB bandwidth are 5 and 7.5 GHz respectively. The probe wavelength is now fixed at 1560.72 nm, and the group delay with the SMF transmission is 85 ps. This means that the inverted probe light is 85 ps later than the Gaussian pulse, and the mixed signal becomes a positive monocycle pulse, as shown in Fig. 7(e). The upper/lower FWHM is 67 ps/90 ps, wider than the FWHM of Fig. 7(a). Therefore, the FWHM of monocycle pulses can be easily adjusted by changing the wavelength span ($\lambda_c - \lambda_s$) or the SMF length. Figure 7(f) shows the corresponding RF spectrum of monocycle pulse in Fig. 7(e). The central frequency and the 10 dB bandwidth are 3.75 and 6.25 GHz respectively.

In this section, a filter-free XGM-based scheme to generate UWB monocycle pulses is proposed. A section of SMF of 2.5 km serves as dispersion medium to induce group delay between the optical Gaussian pulse and the inverted probe light. This feature functions as a two-tap photonic microwave delay-line filter with coefficients of [1, –1], whose frequency response can be optimized to meet the FCC spectrum mask [18]. Both positive and negative monocycle pulses can be obtained depending on the group delay of SMF. This feature enables the realization of PPM when the probe wavelength λ_c is switched on both sides of λ_s, so that the group delay is changed between negative and positive values.

4 All-optical UWB pulse generation based on a hybrid of SPM and XGM

As mentioned in Sect. 3, the Gaussian pulse will be over-amplified at its rising edge after transmitting in the SOA. The pulse distortion results from the SPM in the SOA [28]. Inspired by this property, we obtained UWB monocycle pulses directly from dark Gaussian pulses based on SPM in the SOA [21]. When an optical signal with dark RZ format propagates through the SOA, the rising edge of output signal will be over-amplified and overshot, and the output pulses will become monocycle-like. That scheme has advantages of all-optical operation and single optical source input, without any additional optical filter.

In this section, we extend our previous work in Ref. [21] to generate UWB doublet pulses by injecting an additional probe signal with the SMF transmission. The operational principle is illustrated in Fig. 8. First, the dark RZ pulse at the wavelength λ_s becomes a negative monocycle pulse after propagating in the SOA due to SPM. A CW probe signal at wavelength λ_c then becomes a positive Gaussian pulse after propagating in the SOA due to XGM. A consequent SMF induces the group delay between two input wavelengths (λ_s and λ_c). The time delay is expressed in Eq. (4). As a result, the negative monocycle pulse and the Gaussian pulse will be overlapped by proper time delay to generate a doublet pulse. Our scheme is flexible because the PSM can be easily achieved. The monocycle-doublet conversion can be implemented by just switching the probe light off and on. However, one could not modulate the UWB signal with PPM because only single polar monocycle and doublet pulses are achieved.

The experimental setup is described in Fig. 8. The dark RZ pulse generator consists of the tunable LD 1, an MZM and a BPG. The system has the same configuration as that of Fig. 6, except that the MZM is driven by a different data voltage to form dark RZ pulses. The bit sequence of dark RZ signal is set with a repetition rate of 1.25 GHz. The employed SOA has the same series as that of Sects. 2 and 3. The SOA current is biased at 210 mA. The wavelengths of dark RZ signals and the probe are 1563 and 1560 nm, respectively. The consequent SMF has a length of 1 km with $D = 16.8$ ps/(nm·km), therefore the group delay is −50.4 ps. Another 5 km SMF and 700 m dispersion compensation fiber (DCF) as a dispersion map are used to transmit the doublet pulses without inducing residual dispersion.

First, the LD 2 is switched off to observe monocycle pulses. The FWHM of the input dark RZ pulse is set at 50 ps. When peak power of the input dark RZ signal is 4 mW, the output monocycle pulses are observed. The temporal waveform and its RF spectrum are shown in Figs. 9(a) and 9(b). The upper FWHM and lower FWHM

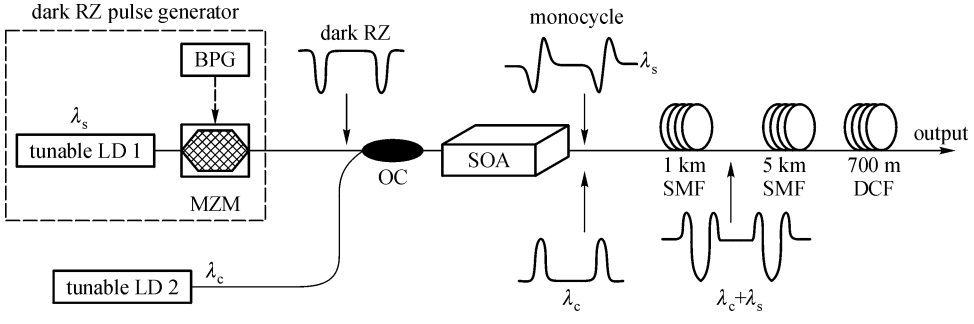

Fig. 8 Experimental setup for all-optical UWB doublet generation based on SPM and XGM

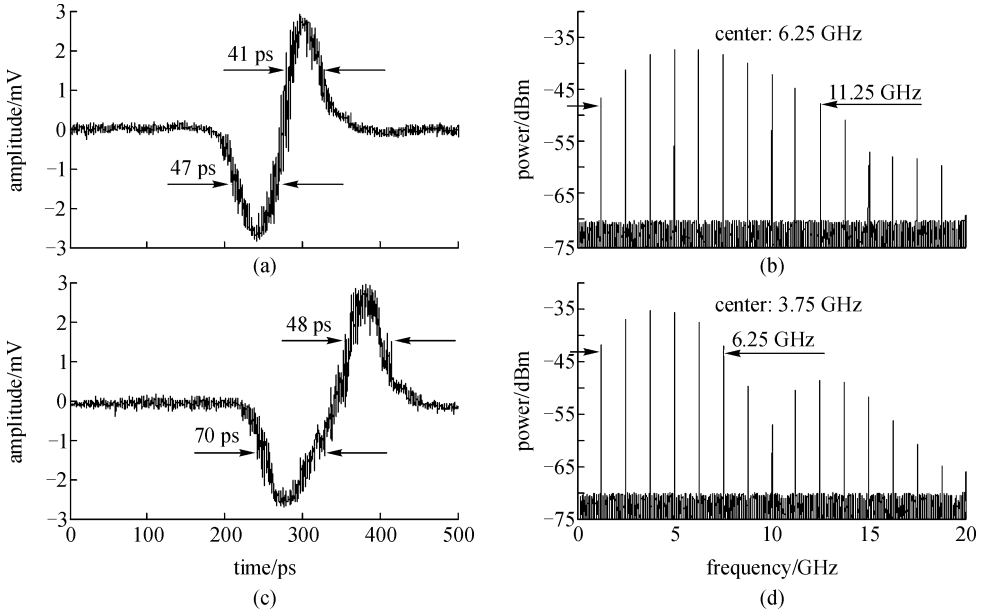

Fig. 9 Measured UWB waveforms and RF spectra. (a) Monocycle pulse (FWHM is 50 ps); (b) RF spectrum (FWHM is 50 ps); (c) monocycle pulse (FWHM is 100 ps); (d) RF spectrum (FWHM is 100 ps)

of monocycle pulse are 41 and 47 ps, respectively. The central frequency and the 10 dB bandwidth are 6.25 and 11.25 GHz, respectively. The FWHM of dark RZ pulse is then set at 100 ps, and the output UWB monocycle pulses are shown in Fig. 9(c). After the measurement, the upper FWHM is 48 ps and the lower FWHM is 70 ps, wider than that of the monocycle in Fig. 9(a). Figure 9(d) shows the RF spectrum corresponding to Fig. 9(c). The spectrum reveals a central frequency of 3.75 GHz and a 10 dB bandwidth of 6.25 GHz, within the UWB definition. Therefore, the FWHM of generated monocycle pulse is controllable via the input FWHM.

When the LD 2 is switched on, it generates a continuous wave (CW) probe light at 1560 nm. The input dark RZ pulse with 60 ps pulsewidth is shown in Fig. 10, denoted as R1. In Fig. 10, R1 is input dark RZ pulse, R2 is the generated positive Gaussian pulse after the SMF, R3 is dark RZ pulse after the SOA, R4 is the generated doublet pulse after 1 km SMF, and R5 is the doublet pulse after 5 km SMF and 700 m transmission. Due to XGM, the probe light becomes a positive Gaussian pulse after propagating in the SOA, as shown in waveform R2. However, the dark RZ pulse becomes monocycle-like due to the overshoot at its rising edge after propagating in the SOA, as shown in waveform R3. The mixed signal with different wavelengths then propagates in the SMF, and the UWB doublet pulse is obtained due to the group delay of SMF, as shown in R4. The probe pulse has a relative delay of about 50.4 ps by SMF dispersion. The generated doublet has a pulse width of 58 ps, and its RF spectrum is shown in Fig. 11(a). The central frequency and 10 dB bandwidth are 7.50 and 8.75 GHz respectively.

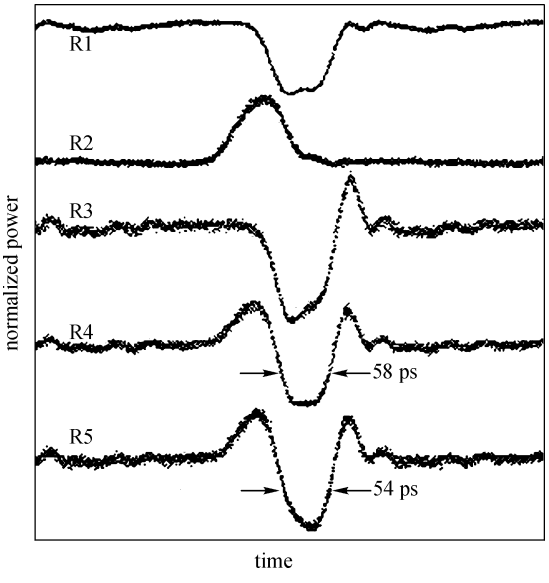

Fig. 10 Evolution of UWB doublet

Since the UWB doublet is generated by combining two channels with different wavelengths, the UWB signal will be distorted when propagating in the optical fiber due to the dispersion effect. Therefore, dispersion management is indispensable when distributing the UWB signals over fiber. A feasible solution is using a periodic dispersion map, which consists of SMF spans and DCF spans. The DCF can totally compensate the residual dispersion of the SMF. As a result, the UWB signal can transmit over fiber without distortion even for widely separated wavelengths. To investigate the transmission property of the

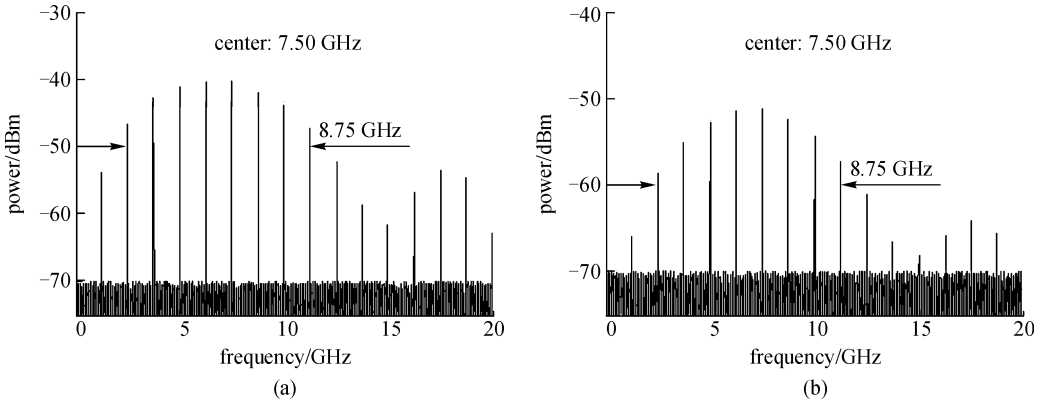

Fig. 11 RF spectra of doublet pulses. (a) Doublet RF spectrum after 1 km SMF; (b) doublet RF spectrum after 5 km SMF and 700 m DCF transmission

doublet pulses, a 5 km SMF is used to transmit the doublet pulses, and a 700 m DCF is used to compensate the residual dispersion between the two wavelengths. The output pulses maintain their doublet shape, as shown in R5 of Fig. 10. The pulse width is 54 ps. The corresponding RF spectrum is shown in Fig. 11(b). One can see that the envelope of UWB spectrum is not changed except for its power attenuation.

From Fig. 9(a), one can see the amplitude-equal monocycle pulse without the probe injection. However, from R3 of Fig. 10, one can see that the upper amplitude of monocycle pulse is smaller than the lower one by probe suppression. This feature ensures that the mixed signal conforms to the standard doublet shape. Hence, in the application of monocycle-doublet conversion, the switching on and off of the LD 2 promote the acquisition of standard doublet and standard monocycle pulses.

5 Conclusion

In this paper, we presented several all-optical methods for UWB pulse generation based on various nonlinear effects of single SOA, namely 1) XPM, 2) XGM, and 3) a hybrid of SPM and XGM. The common feature is all-optical operation, which can be incorporated into UWB-over-fiber networks and simplify the entire network without electrical-optical conversion. Optical advantages such as huge bandwidth capacity and immunity to electromagnetic interference can be utilized by all-optical operation. In addition, the RF spectra of all generated UWB pulses conform to the FCC's UWB definition. From the spectra of doublet and monocycle pulses, one can see that the low-frequency components of a doublet pulse (from 0 to 2.5 GHz) are weaker than those of the monocycle pulse. This is useful to suppress the interference between UWB and other low-frequency communication services such as GPS. The configuration of our all-optical methods is compact and simple. For example, only single SOA and no more than two lasers are required. In the second and third methods, no optical filters and ODL are used, and the SMF serving as a delay device makes the system simple.

Our all-optical methods are feasible for implementing two typical UWB pulse modulation schemes: PSM and PPM. In the first method, one can switch either the probe wavelength or the OBF central wavelength to realize PPM of monocycle pulses. For PPM of doublet pulses, one can use an electrically-controlled ODL to switch the polarity of doublet pulses. The PSM can be implemented when the red shifted OBF is switched off and on. In the second method, the PPM can be realized when the group delay is changed between negative and positive values. In the third method, the PSM can be implemented by just switching the probe light off and on. We also demonstrate non-degraded transmission of UWB doublet pulses over a 5 km SMF.

Acknowledgements This work was supported by the National High Technology Developing Program of China (Grant No. 2006AA03Z0414), the National Natural Science Foundation of China (Grant No. 60407001), and the Science Fund for Distinguished Young Scholars of Hubei Province (Grant No. 2006ABB017).

References

1. Aiello G R, Rogerson G D. Ultra-wideband wireless systems. IEEE Microwave Magazine, 2003, 4(2): 36–47
2. Win M Z, Scholtz R A. Ultra-wide bandwidth time-hopping spread-spectrum impulse radio for wireless multiple-access communications. IEEE Transactions on Communications, 2000, 48(4): 679–689
3. Porcino D, Hirt W. Ultra-wideband radio technology: potential and challenges ahead. IEEE Communications Magazine, 2003, 41(7): 66–74
4. Chen X, Kiaei S. Monocycle shapes for ultra wideband system. In: Proceedings of IEEE International Symposium on Circuits and Systems, 2002, 1, I-597–I-600

5. Kim H, Park D, Joo Y. All-digital low-power CMOS pulse generator for UWB system. Electronics Letters, 2004, 40(24): 1534–1535
6. Bachelet Y, Bourdel S, Gaubert J, Chalopin H. Fully integrated CMOS UWB pulse generator. Electronics Letters, 2006, 42(22): 1277–1278
7. Zhu L, Sun S, Menzel W. Ultra-wideband (UWB) bandpass filters using multiple-mode resonator. IEEE Microwave and Wireless Components Letters, 2005, 15(11): 796–798
8. Kim S, Jang H, Choi S, Kim Y, Jeong J. Performance evaluation for UWB signal transmission with different modulation schemes in multi-cell environment distributed using ROF technology. In: Proceeding of IEEE International Workshop on Ultra Wideband Systems, 2004, 187–191
9. Lin W, Chen J. Implementation of a new ultrawide-band impulse system. IEEE Photonics Technology Letters, 2005, 17(11): 2418–2420
10. Zeng F, Yao J. Ultrawideband impulse radio signal generation using a high-speed electrooptic phase modulator and a fiber-Bragg-grating-based frequency discriminator. IEEE Photonics Technology Letters, 2006, 18(19): 2062–2064
11. Kawanishi T, Sakamoto T, Izutsu M. Ultra-wide-band signal generation using high-speed optical frequency-shift-keying technique. In: 2004 IEEE International Topical Meeting on Microwave Photonics, 2004, 48–51
12. Chen H, Chen M, Qiu C, Zhang J, Xie S. UWB monocycle pulse generation by optical polarisation time delay method. Electronics Letters, 2007, 43(9): 542–543
13. Zeng F, Yao J. An approach to ultrawideband pulse generation and distribution over optical fiber. IEEE Photonics Technology Letters, 2006, 18(7): 823–825
14. Torres-Company V, Prince K, Monroy I T. Fiber transmission and generation of ultrawideband pulses by direct current modulation of semiconductor lasers and chirp-to-intensity conversion. Optics Letters, 2008, 33(3): 222–224
15. Wang Q, Yao J. UWB doublet generation using nonlinearly-biased electro-optic intensity modulator. Electronics Letters, 2006, 42(22): 1304–1305
16. Dong J J, Zhang X L, Xu J, Huang D X, Fu S N, Shum P. High order ultrawideband pulse generation from NRZ-DPSK signals. In: Proceedings of Conference on Optical Fiber Communication/ National Fiber Optic Engineers Conference (OFC/NFOEC 2008). San Diego: IEEE, 2008, 1–3
17. Li J, Xu K, Fu S, Wu J, Lin J, Tang M, Shum P. Ultra-wideband pulse generation with flexible pulse shape and polarity control using a Sagnac-interferometer-based intensity modulator. Optics Express, 2007, 15(26): 18156–18161
18. Yao J, Zeng F, Wang Q. Photonic generation of ultrawideband signals. Journal of Lightwave Technology, 2007, 25(11): 3219–3235
19. Wang Q, Zeng F, Blais S, Yao J. Optical ultrawideband monocycle pulse generation based on cross-gain modulation in a semiconductor optical amplifier. Optics Letters, 2006, 31(21): 3083–3085
20. Dong J J, Zhang X L, Xu J, Huang D X, Fu S N, Shum P. Ultrawideband monocycle generation using cross phase modulation in a semiconductor optical amplifier. Optics Letters, 2007, 32(10): 1223–1225
21. Dong J J, Zhang X L, Xu J, Huang D X. All-optical ultrawideband monocycle generation utilizing gain saturation of a dark return-to-zero signal in a semiconductor optical amplifier. Optics Letters, 2007, 32(15): 2158–2160
22. Dong J J, Zhang X L, Xu J, Huang D X. Filter-free ultrawideband generation based on semiconductor optical amplifier nonlinearities. Optics Communications, 2008, 281(4): 808–813
23. Zeng F, Wang Q, Yao J. All-optical UWB impulse generation based on cross-phase modulation and frequency discrimination. Electronics Letters, 2007, 43(2): 121–122
24. Wang C, Zeng F, Yao J. All-fiber ultrawideband pulse generation based on spectral shaping and dispersion-induced frequency-to-time conversion. IEEE Photonics Technology Letters, 2007, 19(3): 137–139
25. Wang Q, Yao J. An electrically switchable optical ultrawideband pulse generator. Journal of Lightwave Technology, 2007, 25(11): 3626–3633
26. Lin W, Chen Y. Design of a new optical impulse radio system for ultra-wideband wireless communications. IEEE Journal of Selected Topics Quantum Electronics, 2006, 12(4): 882–887
27. Xu J, Zhang X L, Dong J J, Liu D M, Huang D X. High-speed all-optical differentiator based on a semiconductor optical amplifier and an optical filter. Optics Letters, 2007, 32(13): 1872–1874
28. Agrawal G P, Olsson N A. Self-phase modulation and spectral broadening of optical pulses in semiconductor laser amplifiers. IEEE Journal of Quantum Electronics, 1989, 25(11): 2297–2306